FABRICATION AND MAGNETIC FIELD MEASUREMENT OF AN APPLE-2 TYPE VARIABLE POLARIZING UNDULATOR

KAKUNO Kazunori, KOBAYASHI Hideki, OHASHI Ken,
Shin-Etsu Chemical Co., Ltd., Takefu, Fukui, Japan
BIZEN Teruhiko, HIRAMATSU Yoichi, MIYAHARA Yoshikazu and SHIMADA Taihei,
SPring-8, Mikazuki, Sayu-gun, Hyogo, Japan

Abstract

This report presents fabrication and field measurement of an APPLE-2 type variable polarizing undulator for SPring-8.

1 INTRODUCTION

A variable polarizing undulator (ID23)[1] as the light source of the soft X-ray beamline (BL23SU)[2] for SPring-8 has been constructed. The magnetic structure of the ID23 is APPLE-2 type[3-5]. The ID23 can generate a linearly (horizontal or vertical plane), an elliptically or a circularly polarized radiation by providing the phase position shifts to the magnet rows of the undulator. The most important performance of the ID23 is switching of right and left circularly polarized radiation at 0.5Hz by successful phase shift driving of the magnet rows. This feature is expected to promote a study of circular dichroism in spectroscopic research fields. Main parameters of the ID23 are shown in Table 1. We have made some change of the design reported on EPAC'96[1] as in the process the construction.

Table 1: Main parameters of the ID23

Device type	APPLE-2
Period length	120 mm
Period number	16
Available gap range	20~300 mm
Available phase shift range	-120~+120 mm
Switching rate (right~left~right)	0.5 Hz
Peak field for horizontal polarization	$By=0.55$ T
Peak field for vertical polarization	$Bx=0.55$ T
Peak field for circular polarization	$By=Bx=0.39$ T

2 TOLERANCE OF FIELD ERROR

Since errors of the magnetic field of the insertion device deteriorate the characteristic of the radiation from the insertion device and distort the closed orbit (CO) of the electron beam, the errors must be minimized. We have considered the tolerance for the errors. The tolerance are defined at the gap=30mm, at the phase position for vertical and horizontal polarization.
1) The tolerance of the deviation of the integral field as follows:

$$\frac{\sigma(BL)}{m(BL)} < 0.5\%$$

where $\sigma(BL)$ is a standard deviation of BLi, $m(BL)$ is a mean of BLi, where BLi is a field integral along the orbit per a half period as follows:

$$BLi = \left| \int_{Li}^{Li+1} B ds \right|$$

where B is the magnetic field, Li is position of B crossing zero. This value determines a deviation of the periodic motion of the electron beam in the field of the insertion device.
2) The tolerance of the maximum difference between the mean actual orbit and the mean ideal orbit is an amplitude of the sinusoidal orbit shown in Figure 1. This value determines an increase in the divergence of the radiation from the insertion device.
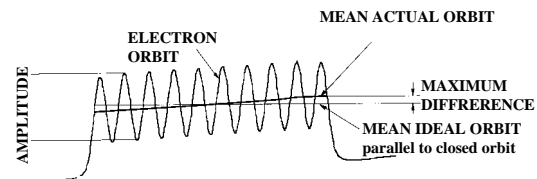

Figure 1: Error of electron orbit

3) The tolerance of the integral field along the orbit is 100 Gcm as follows:

$$\left| \int_0^L B ds \right| < 100 \, Gcm$$

where s=0 is at an upstream of 300mm from the entrance of the magnetic structure and s=L is at a downstream of 300 mm from the exit. This value determines the error kick to the CO.

3 FABRICATION OF MAGNETIC STRUCTURE

The magnetic structure of the ID23 consists of four permanent magnet rows. Each row is divided into two units 1 m long to be easy to handle.

Figure 2 shows a cross sectional view of the row. Main elements of the magnetic structure are permanent magnet pieces, holders and base plates. We have specified the relative magnetic permeability of the materials of the all elements to be close to 1.0 for the reduction of the distortion of the field. The magnet pieces are fixed by not adhesive but full metal parts only to be free radiation damage. Specifications of the main elements is shown in Table 2.

Table 2: Specifications of the main elements

Permanent magnet piece
Material	alloy of Nd-Fe-B (N36H)[7]
Number (total of the ID23)	260
normal type (vertical magnetization)	124
normal type (longitudinal magnetization)	128
end type (vertical magnetization)	8
Size of normal type piece	W50H25L30mm^3
Size of end type magnet	W50H25L15mm^3
Remanent field	1.2 T
Deviation of direction of magnetization	<1°
Deviation of strength of magnetization	<1%
Surface coarting	8~15mm thickness of Ni

Holder
Material	non magnetic stainless steel; SUS304
Number (total of the ID23)	260
normal type	252
end type	8

Base plate
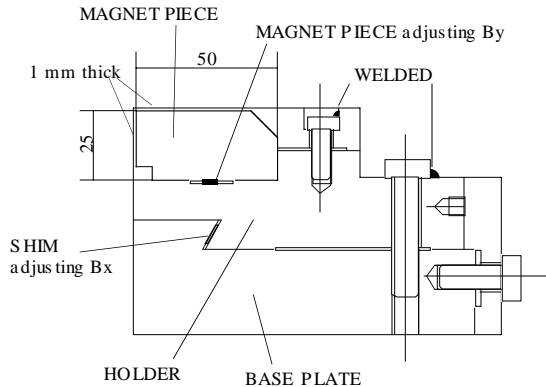|	
Material	non magnetic stainless steel; SUS304
Number (total of the ID23)	8

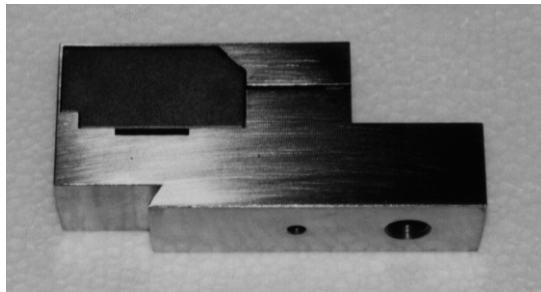Figure 2: Cross section view of permanent magnet row

Figure 3: Permanent magnet piece in holder

One holder fixes one magnet piece shown in Figure 3. The holders including the magnet pieces are fixed on the base plate as shown in Figure 4. Since it is dangerous to the vacuum chamber of the storage ring if the magnet pieces are broken during the phase shift motion at the minimum gap, the holders cover the magnet pieces completely.

We have welded the bolts fixing the magnet piece to the holder and the holders to the base plate after the adjustment of the field. Because we fear that the bolts become loose due to the vibration during phase shift motion repeating at 0.5 Hz. We measured the change of the field by the welding, which was not detected.
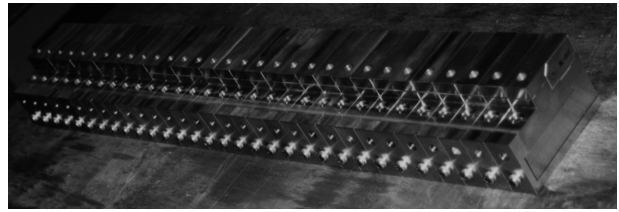

Figure 4: Magnet pieces in holder on base plate

4 ADJUSTMENT IF FIELD DISTRIBUTION

In an APPLE-type undulator, on-axis magnetic field change by phase shift on two pairs of magnet rows. In order to satisfy the specification about magnetic field on any phase mode, we had adjusted the field of one pair of rows and that of other pair individually. Because the on-axis field of one pair of rows is skewed, horizontal field Bx and vertical one By were adjusted independently.

First we had assembled the magnet rows after magnet sorting about Bx in which measurement data of open flux of each magnet was used. The second integral distribution of the on-axis field after sorting is shown in Figure 5, the effect of sorting about Bx appears. Secondly, we measured the field of one pair of rows and calculated field-integral of each half-period to correct unevenness of each field-integral. In order to correct the field, we shifted magnet position. Bx was corrected by shifting magnet position in y-direction and By in x-direction. Distance of magnet shifting was about 0.1mm to 0.3mm. The second integral after this correction is shown in Figure 6 and field error has removed considerably. Finally, after two pairs of rows ware attached on support unit, the kick of electron trajectory at entrance and exit of undulator were corrected by magnet shifting. As shown in Figure 7~9, considerable field error sake not seen at any phase mode.

5 MEASUREMENT OF FIELD

The field distribution along the orbit was measured using a Hall effect device. In order to minimize the planar Hall effect[8] which obstructs the measurement in case of the phase position for elliptically polarization, we set the direction of the driving current of the Hall plate to Z-direction in measurement both By and Bx[9] on the assumption that Bz=0, where XYZ coordinates is a right hand system. Figure 7~9 shows results of the measurement of the field distribution.

The integral field was measured using a long flip coil. Results are shown in Figure 10(1).

6 DISCUSSION AND CONCLUSION

The field distribution satisfies the tolerance at gap=30mm.

In order to minimize the closed orbit distortion induced by residual errors of the integral field, we must adjust the current set of some collecting magnets associated with the ID23 for the function as the gap and phase position.

The integral field varies with the phase motion at the fixed gap shown in Figure 10(2). We consider the reasons as follows; relative magnetic permeability of the elements especially the magnet pieces are not exactly 1, the variation of the magnetic force between the magnet pieces due to the phase motion distorts the magnet structure.

7 ACKNOWLEDGMENT
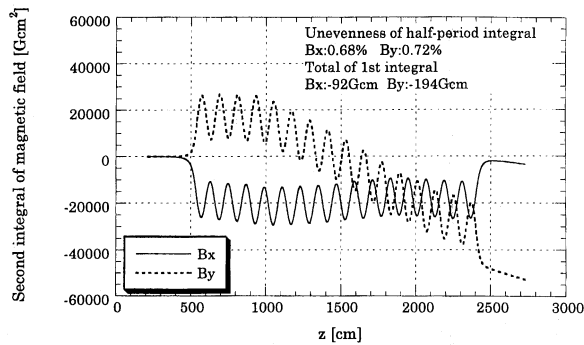
Figure 5: Second integral distribution of on-axis magnetic field after sorting at gap=30mm
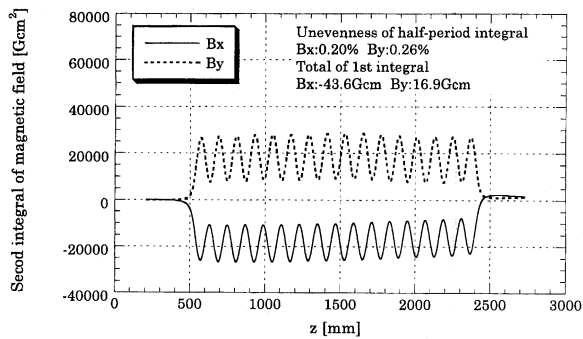

Figure 6: Second integral distribution of on-axis magnetic field after field correction at gap=30mm
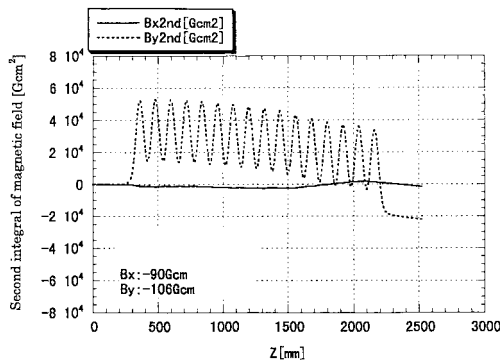

Figure 7: Second integral distribution of on-axis magnetic field for horizontal polarization at gap=30mm
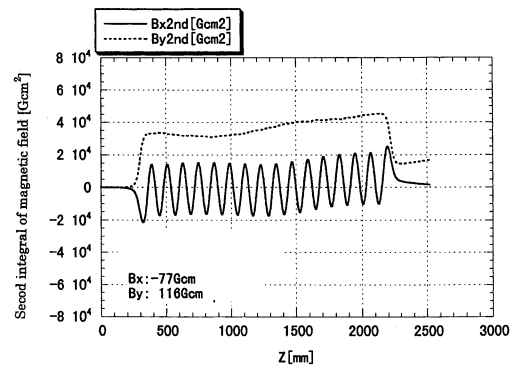

Figure 8: Second integral distribution of on-axis magnetic field for vertical polarization at gap=30mm
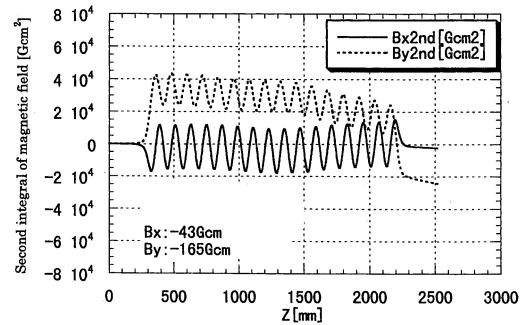

Figure 9: Second integral distribution of on-axis magnetic field for near circulay polarization at gap=30mm
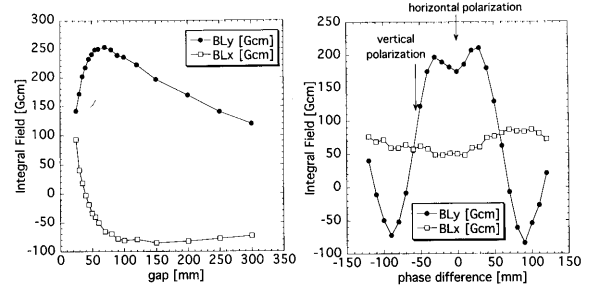

Figure 10(1): Integral field at phase=0mm

Figure 10(2): Integral field at gap=30mm

REFERENCES

[1] H.KOBAYASHI, et al., EPAC'96, 2579-2581.
[2] A.YOKOYA, et al.,
     J.Synchrotron Rad. (1998)5,10~16.
[3] S.SASAKI, et al.,
     Jpn.J.Appl.Phys.,Vol.31, L1794(1992).
[4] S.SASAKI, et al., NIM. A331(1993)763-767.
[5] S.SASAKI, NIM A347(1994)83-86.
[6] T..SHIMADA et al., EPAC'98.
[7] Shin-Etsu Chemical Co., Ltd.,
     Catalogue of Shin-Etsu Rare Earth Magnets.
[8] M.W.Pool et al., IEEE TRANS. MAGNETICS,
     VOL.MAG-17, NO.5, SEPTEMBER 1981.
[9] M.TURIN, NIM.91(1971)621-625.